Available online at www.sciencedirect.com
ScienceDirect
Polymer 48 (2007) 3664–3672
polymer
www.elsevier.com/locate/polymer

Synthesis and characterization of side-chain liquid crystalline homopolymers and block copolymers containing biphenyl-4-ylthiophene and biphenyl-4-ylfluorene pendants

Kuan-Wei Lee, Hong-Cheu Lin*

Department of Materials Science and Engineering, National Chiao Tung University, Hsinchu, Taiwan, ROC

Received 16 March 2007; received in revised form 23 April 2007; accepted 24 April 2007
Available online 29 April 2007

Abstract

A series of new liquid crystalline homopolymers (**P1** and **P2**) and block copolymers (**P3** and **P4**) composed of methacrylates containing pendant biphenyl-4-ylthiophene (**M1**) and biphenyl-4-ylfluorene (**M2**) units were synthesized by atom transfer radical polymerization (ATRP). The number-average molecular weights (M_n) of the homopolymer (**P2**) and diblock copolymers (**P3** and **P4**) were in the range of 5153–8713 g mol^{-1} with polydispersity indices (PDIs) between 1.17 and 1.25. The thermal, mesogenic, and photoluminescence (PL) properties of all polymers were investigated. Except for the absence of mesogenic properties in block copolymer **P4**, polymers **P1** and **P3** possessed the smectic A phase and polymer **P2** exhibited the nematic phase. Moreover, the mesomorphism and the layer *d*-spacing values of the smectic A phase in polymers **P1** and **P3** were confirmed and characterized by X-ray diffraction (XRD) patterns.

Keywords: Block copolymer; Atom transfer radical polymerization (ATRP); Mesogenic properties

1. Introduction

A wide variety of liquid crystalline (LC) copolymers [1–7] with optimized structures have been developed in recent years. In addition, numerous liquid crystalline (LC) block copolymers consisting of mesogenic blocks and isotropic blocks were synthesized via different types of living free-radical polymerization [8–11] and their phase behavior and morphology were characterized. In general, there are two kinds of LC block copolymers, i.e. main-chain and side-chain LC block copolymers, where mesogenic groups connected along the backbones are main-chain copolymers (such as copolyesters composed of *p*-hydroxybenzoic acid and poly(ethylene terephthalate), etc.) [12–14], and pendant mesogenic groups attached to the backbones via flexible spacers are side-chain copolymers.

Among these LC copolymers, side-chain LC copolymers have attracted significant interests because of their liquid crystalline behavior as low molecular mass pendant mesogens and their easy processing characteristic as polymers. Furthermore, side-chain LC polymers are often used in electro-optical applications due to their lower viscosities and easier alignment tendencies than those of main-chain LC polymers. Several kinds of rigid cores, including azobenzene [15–17] and biphenyl units [18–23], were applied to mesogenic groups of side-chain LC polymers. In our previous research [24], side-chain LC polymers containing cyanoterphenyl units were also reported to possess mesogenic phases and high stabilities in thermal, chemical, and photochemical properties, but they had poor solubilities. Herein, in order to improve solubility, a series of new mesogenic homopolymers and block copolymers composed of methacrylates containing pendant biphenyl-4-ylthiophene (**M1**) and biphenyl-4-ylfluorene (**M2**) groups were synthesized by atom transfer radical polymerization (ATRP), where block copolymers **P3** and **P4** were produced from styrene macroinitiator (**SMi**). Furthermore, the thermal, mesogenic,

* Corresponding author. Tel.: +886 3 5712121x55305; fax: +886 3 5724727.
E-mail address: linhc@cc.nctu.edu.tw (H.-C. Lin).

0032-3861/$ - see front matter © 2007 Elsevier Ltd. All rights reserved.
doi:10.1016/j.polymer.2007.04.057

and photoluminscent (PL) properties of all polymers were also investigated in this study.

2. Experimental

2.1. Measurements

^{1}H NMR spectra were recorded on a Varian unity 300 MHz spectrometer using $CDCl_3$ and d_6-DMSO solvents. Elemental analyses were performed on a HERAEUS CHN-OS RAPID elemental analyzer. Transition temperatures were determined by differential scanning calorimetry (DSC) (Perkin–Elmer, model: Diamond) with heating and cooling rates of 5 °C/min. The mesomorphic properties were studied using a polarizing optical microscope (POM) (Leica, model: DMLP) equipped with a hot stage. Thermogravimetric analysis (TGA) was conducted on a Du Pont Thermal Analyst 2100 system with a TGA 2950 thermogravimetric analyzer at a heating rate of 10 °C/min under nitrogen. Gel permeation chromatographic (GPC) analysis was conducted on a Waters 1515 separation module with chloroform as the eluant against a polystyrene calibration curve. UV–visible absorption spectra were recorded in dilute THF solutions (10^{-6} M) on a HP G1103A spectrophotometer. Photoluminescence (PL) spectra were obtained on a Hitachi F-4500 spectrophotometer.

2.2. Materials

Unless otherwise specified, chemicals and solvents were of reagent grade and purchased from Aldrich, Acros, TCI, and Lancaster Chemical Co. Dichloromethane and THF were distilled to keep it anhydrous before use. Pyridine was dried by refluxing over calcium hydride. The other chemicals were used without further purification.

2.3. Syntheses of monomers

The synthetic routes of monomers (**M1** and **M2**) and the macroinitiator (**SMi**) are shown in Scheme 1. Their synthetic details were described as follows.

2.3.1. 4-Bromo-4′-octoxybiphenyl (*2*)

1-Bromooctane (11.6 g, 60 mmol), 4-bromo-4′-hydroxybiphenyl (**1**) (10 g, 40 mmol), and potassium carbonate (16.6 g, 120 mmol) were dissolved in butan-2-one (100 mL) and reacted under reflux for 24 h. After cooling to room temperature, the potassium salt was filtered off. The solvent was removed by rotavapor and the crude product was recrystallized from petroleum ether (bp: 35–60 °C) to yield a white solid (13.5 g, 93%). ^{1}H NMR (ppm, $CDCl_3$) δ: 0.89 (t, $J = 6.9$ Hz, 3H), 1.29–1.47 (m, 10H), 1.80 (quintet, $J = 6.6$ Hz, 2H), 3.98 (t, $J = 8.6$ Hz, 2H), 6.99 (d, $J = 8.8$ Hz, 2H), 7.40–7.54 (m, 6H) [24].

2.3.2. 4′-Octoxybiphenyl-4-ylboronic acid (*3*)

4-Bromo-4′-octoxybiphenyl (**2**) (5 g, 13.8 mmol) was dissolved in THF (200 mL) and then *n*-butyllithium (8.9 mL, 2.5 M, 22.1 mmol) was added dropwise to react at −78 °C. The reaction mixture was maintained under this condition for 1 h. Furthermore, it was added dropwise to trimethyl borate solution (3.5 g, 33.2 mmol) at −78 °C. The solution was allowed to cool to room temperature overnight, and the final solution was acidified with 100 mL of 10% HCl solution and stirred for 45 min at room temperature. Subsequently, the solution was washed with saturated sodium carbonate solution and water, and then THF was removed. The crude product was extracted by diethyl ether and the organic layer was dried over magnesium sulfate. After removing the solvent by rotavapor, the resulting solid was washed with petroleum ether and briefly dried on filter to obtain a white solid (6.0 g, 80%). ^{1}H NMR (ppm, d_6-DMSO) δ: 0.85 (t, $J = 7.2$ Hz, 3H), 1.24–1.41 (m, 10H), 1.71 (quintet, $J = 6.6$ Hz, 2H), 3.98 (t, $J = 6.6$ Hz, 2H), 6.99 (d, $J = 8.8$ Hz, 2H), 7.56–7.62 (m, 4H), 7.83 (d, $J = 8.8$ Hz, 2H), 8.03 (s, 2H) [24].

2.3.3. 2-(4′-Octoxy-biphenyl-4-yl)-thiophene (*6*)

Compound **4** (3 g, 18.5 mmol), compound **3** (7.9 g, 24.1 mmol), and tetrakis(triphenylphosphine)palladium(0) (1.07 g, 0.93 mmol) were reacted in THF (200 mL) for 10 min, and then 130 mL of 2 M aqueous Na_2CO_3 solution was added. The mixture was reacted and refluxed for 48 h. After reaction, the cooled solution was washed with dilute hydrochloric acid (10%) and water, and dried over magnesium sulfate. The final solution was purified by column chromatography (silica gel, CH_2Cl_2/hexane 1:1) to yield a white solid (4.8 g, 71%). ^{1}H NMR (ppm, $CDCl_3$) δ: 0.87 (t, $J = 6.9$ Hz, 3H), 1.27–1.45 (m, 10H), 1.81 (quintet, $J = 6.3$ Hz, 2H), 3.97 (t, $J = 6.6$ Hz, 2H), 6.92 (d, $J = 9.6$ Hz, 2H), 7.06 (dd, $J = 3.6$ Hz, 1H), 7.26 (d, $J = 5.4$ Hz, 1H), 7.31 (d, $J = 3.6$ Hz, 1H), 7.51 (m, 4H), 7.63 (d, $J = 8.7$ Hz, 2H).

2.3.4. 2-(4′-Octoxy-biphenyl-4-yl)-9,9-diethyl-9H-fluorene (*7*)

Compound **7** was synthesized by means of analogous procedures of compound **6** via Suzuki coupling reaction. Yield: 71%. ^{1}H NMR (ppm, $CDCl_3$) δ: 0.34 (t, $J = 6.6$ Hz, 6H), 0.85 (t, $J = 6.9$ Hz, 3H), 1.27–1.45 (m, 10H), 1.83 (quintet, $J = 6.6$ Hz, 2H), 2.09 (m, 4H), 3.98 (t, $J = 6.3$ Hz, 2H), 6.96 (d, $J = 8.7$ Hz, 2H), 7.29–7.35 (m, 3H), 7.54–7.75 (m, 10H).

2.3.5. 2-(4′-Hydroxyl-biphenyl-4-yl)-thiophene (*8*)

2-(4′-Octoxy-biphenyl-4-yl)-thiophene (**6**) (4.6 g, 12.6 mmol) was dissolved in dry chloroform (150 mL) under nitrogen and then boron tribromide (6.4 g, 25.2 mmol) was added dropwise to react at −78 °C. The mixture was allowed to warm up to room temperature and reacted for 24 h. The solution was washed with sodium hydroxide (1 M, 50 mL) and then was acidified with 10% HCl and stirred for 4 h. Finally, the suspension was filtered off and purified by column chromatography (silica gel, ethyl acetate) to yield a white solid (2.8 g, 89%). ^{1}H NMR (ppm, d_6-DMSO) δ: 6.85 (d, $J = 8.4$ Hz, 2H), 7.14 (dd, $J = 3.9$ Hz, 1H), 7.50 (d, $J = 4.0$ Hz, 1H), 7.54 (d, $J = 3.6$ Hz, 1H), 7.60 (m, 4H), 7.68 (d, $J = 8.4$ Hz, 2H), 9.56 (s, 1H).

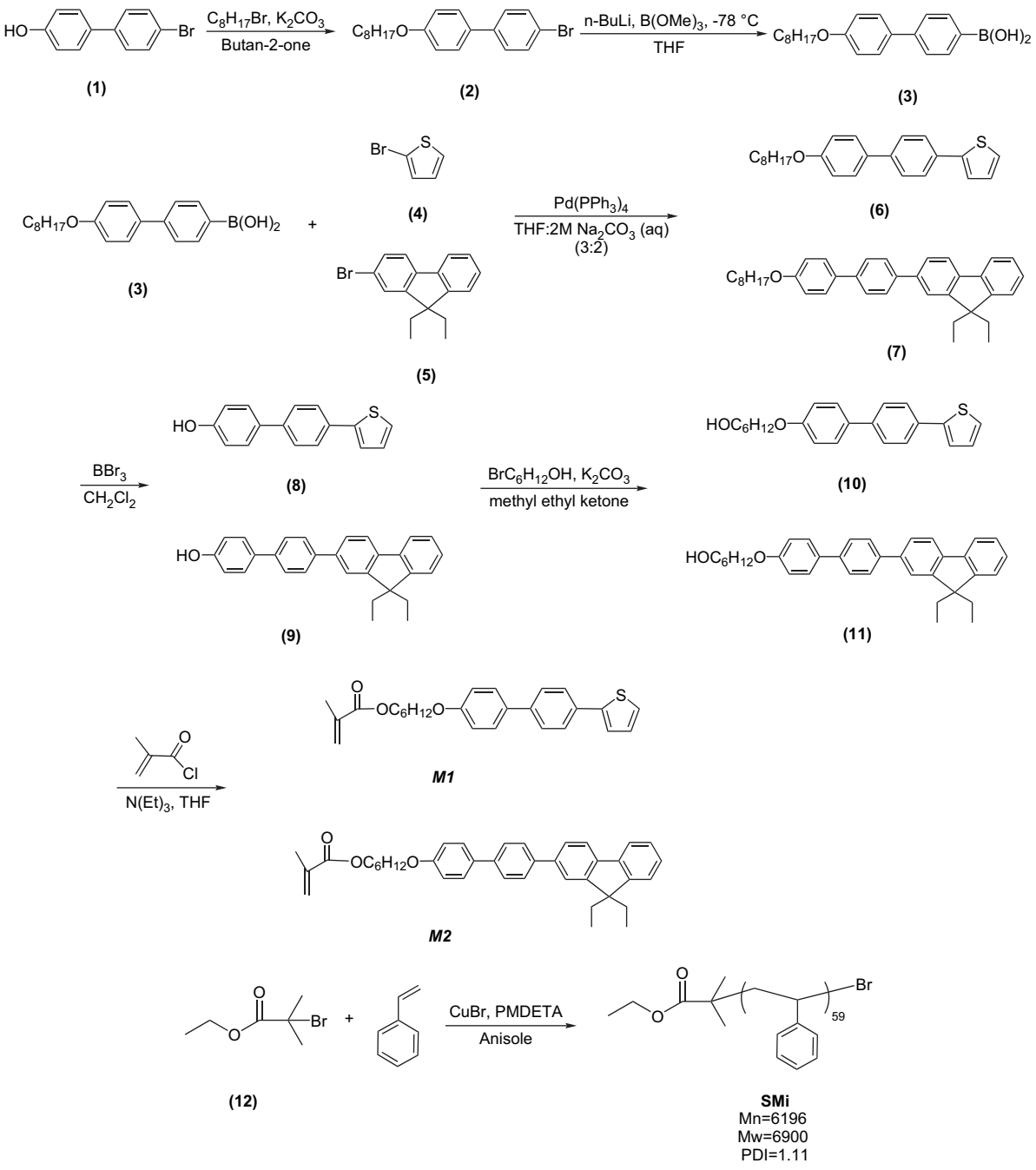

Scheme 1. Synthetic routes of monomers (**M1** and **M2**) and the macroinitiator (**SMi**).

*2.3.6. 2-(4′-Hydroxyl-biphenyl-4-yl)-9,9-diethyl-9H-fluorene (**9**)*

Compound **9** was synthesized through analogous procedures of compound **8**. Yield: 87%. ^{1}H NMR (ppm, d_6-DMSO) δ: 0.35 (t, $J = 7.2$ Hz, 6H), 2.07 (m, 4H), 6.58 (s, 1H), 6.94 (d, $J = 8.4$ Hz, 2H), 7.31–7.33 (m, 3H), 7.50–7.76 (m, 10H).

*2.3.7. 2-(4′-(6-Hydroxyhexyloxy)-biphenyl-4-yl)-thiophene (**10**)*

Compound **8** (2.5 g, 9.9 mmol), 6-chloro-1-hexanol (2.3 g, 12.9 mmol), K_2CO_3 (4.1 g, 29.7 mmol), and KI (20 mg) were dissolved in 200 mL of DMF to reflux overnight. The reaction mixture was then cooled and poured into 200 mL of water and stirred for 2 h. The crude product was extracted with ethyl acetate and the organic layers were washed with a saturated aqueous solution of NaCl and water, and then the organic layer was dried over magnesium sulfate. After removing the solvent by rotavapor, the residue was recrystallized from absolute ethanol to give a colorless solid (2.4 g, 69%). ^{1}H NMR (ppm, d_6-DMSO) δ: 1.22–1.70 (m, 8H), 3.39 (m, 2H), 3.99 (t, $J = 6.4$ Hz, 2H), 4.35 (t, $J = 5.1$ Hz, 1H), 7.00 (d, $J = 9.0$ Hz, 2H), 7.14 (dd, $J = 3.9$ Hz, 1H), 7.53 (d, $J = 4.8$ Hz, 1H), 7.55 (d, $J = 3.6$ Hz, 1H), 7.64 (m, 4H), 7.70 (d, $J = 8.7$ Hz, 2H).

*2.3.8. 2-(4′-(6-Hydroxyhexyloxy)-biphenyl-4-yl)-9,9-diethyl-9H-fluorene (**11**)*

Compound **11** was synthesized via analogous procedures of compound **10**. Yield: 80%. ^{1}H NMR (ppm, $CDCl_3$) δ: 0.35 (t, $J = 7.2$ Hz, 6H), 1.41–1.83 (m, 8H), 2.10 (m, 4H), 3.65 (m, 2H), 4.00 (t, $J = 6.4$ Hz, 2H), 6.97 (d, $J = 9.0$ Hz, 2H), 7.30–7.35 (m, 3H), 7.54–7.76 (m, 10H).

*2.3.9. **M1***

2-(4′-(6-Hydroxyhexyloxy)-biphenyl-4-yl)-thiophene (**10**) (2.0 g, 5.7 mmol), triethylamine (5.7 g, 57 mmol), and 2,6-di-tertbutyl-4-methylphenol (100 mg, as a thermal inhibitor) were dissolved in 150 mL of anhydrous THF under a nitrogen atmosphere and then methacryloyl chloride (1.8 g, 17.1 mmol) was added dropwise. Afterward, the reaction mixture was heated under reflux overnight and then cooled to pour into 200 mL of aqueous NH_4Cl solution (10%). The crude product was extracted with CH_2Cl_2. The resulting organic layer was washed with a saturated solution of NaCl and water, and the organic layer was dried over magnesium sulfate. After removing the solvent by rotavapor, the resulting solid was purified by column chromatography using dichloromethane as an eluant to yield a colorless solid (1.9 g, 81%). ^{1}H NMR (ppm, $CDCl_3$) δ: 1.45–1.50 (m, 4H), 1.67–1.84 (m, 4H), 1.93 (s, 3H), 3.99 (t, $J = 6.5$ Hz, 2H), 4.15 (t, $J = 6.6$ Hz, 2H), 5.53 (s, 1H), 6.09 (s, 1H), 6.96 (d, $J = 9.0$ Hz, 2H), 7.07 (dd, $J = 3.6$ Hz, 1H), 7.26 (d, $J = 5.1$ Hz, 1H), 7.32 (d, $J = 3.6$ Hz, 1H), 7.54 (m, 4H), 7.64 (d, $J = 8.7$ Hz, 2H). Elemental analysis for $C_{26}H_{28}O_3S$: Calc. C, 74.25; H, 6.71; found C, 74.43; H, 6.76. HRMS (EI) *m/z*: Calc. 420.1759; found 420.1754.

*2.3.10. **M2***

Monomer **M2** was synthesized by analogous procedures of **M1**. Yield: 83%. ^{1}H NMR (ppm, $CDCl_3$) δ: 0.36 (t, $J = 6.9$ Hz, 6H), 1.45–1.56 (m, 4H), 1.67–1.83 (m, 4H), 1.94 (s, 3H), 2.06 (m, 4H), 4.01 (t, $J = 6.3$ Hz, 2H), 4.16 (t, $J = 6.6$ Hz, 2H), 5.54 (s, 1H), 6.09 (s, 1H), 6.98 (d, $J = 8.7$ Hz, 2H), 7.32–7.36 (m, 3H), 7.55–7.77 (m, 10H). Elemental analysis for $C_{39}H_{42}O_3$: Calc. C, 83.83; H, 7.58; found C, 83.52; H, 7.54. HRMS (EI) *m/z*: Calc. 558.3134; found 558.3126.

2.4. Polymerization

*2.4.1. Macroinitiator (**SMi**)*

In a Schlenk flask, *N*,*N*,*N*′,*N*′,*N*″-pentamethyldiethylenetriamine (PMDETA, 3.46 mg, 0.5 mmol), CuBr (14.3 mg, 0.25 mmol), and styrene (6.8 g, 65 mmol) were added and stirred for 30 min. Ethyl 2-bromo-2-methylpropanoate (195 mg, 1 mmol) was added, and the mixture was immediately frozen in liquid nitrogen under vacuum. After several freeze–thaw cycles, the flask was sealed under vacuum and put in an oil bath at 100 °C to react for 20 h. After reaction, the content was dissolved in chloroform. After being concentrated, the chloroform solution was precipitated into methanol and the precipitation was repeated for three times. The final product was dried at 50 °C under vacuum. Yield: 75%. The number-average molecular weight measured by GPC was $M_n = 6196$ g mol^{-1} with PDI (M_w/M_n) = 1.11.

*2.4.2. Preparation of homopolymers (**P1** and **P2**) and block copolymers (**P3** and **P4**)*

According to analogous procedures as shown in Scheme 2, homopolymers (**P1** and **P2**) and block copolymers (**P3** and **P4**) were synthesized by utilization of initiators **12** and **SMi**, respectively.

*2.4.2.1. **P1***. Yield: 80 mg (36%). *N*,*N*,*N*′,*N*′,*N*″-Pentamethyldiethylenetriamine (PMDETA, 8.7 mg, 0.05 mmol), CuBr (3.6 mg, 0.025 mmol), and **M1** (210.3 mg, 0.5 mmol) were added and stirred for 30 min. After that, ethyl 2-bromo-2-methylpropanoate (**12**) (1.95 mg, 0.01 mmol) was added, and the mixture was immediately frozen in liquid nitrogen under vacuum. The mixture was degassed three times using the freeze–pump–thaw procedure and sealed under vacuum. After stirring for 30 min at room temperature, the mixture was reacted at 100 °C in a preheated oil bath for 24 h. The mixture was reprecipitated more than twice in methanol and then washed by acetone. A white product of polymer was collected by filtration and dried under vacuum. By analogous procedures, ^{1}H NMR data, and GPC results of the other homopolymer and copolymers are listed as follows.

*2.4.2.2. **P2***. Yield: 75 mg (27%). ^{1}H NMR (ppm, $CDCl_3$) δ: 0.31 (broad), 0.93 (broad), 1.53–1.93 (broad), 2.02 (broad), 3.97 (broad), 6.91 (broad), 7.29 (broad), 7.54 (broad). The number-average molecular weight measured by GPC was $M_n = 5103$ g mol^{-1} with PDI (M_w/M_n) = 1.25.

*2.4.2.3. **P3** (monomer/initiator = 30/1)*. Yield: 110 mg (40%). ^{1}H NMR (ppm, $CDCl_3$) δ: 0.96 (broad), 1.41–1.93 (broad), 3.99 (broad), 6.55 (broad), 7.06 (broad), 7.31 (broad), 7.59 (broad). The number-average molecular weight of the soluble part of the polymer measured by GPC was $M_n = 8713$ g mol^{-1} with PDI (M_w/M_n) = 1.19.

*2.4.2.4. **P4** (monomer/initiator = 30/1)*. Yield: 100 mg (29%). ^{1}H NMR (ppm, $CDCl_3$) δ: 0.30 (broad), 0.85 (broad), 1.40–1.84 (broad), 2.03 (broad), 3.98 (broad), 6.55 (broad), 7.02 (broad), 730 (broad), 7.58 (broad). The number-average molecular weight measured by GPC was $M_n = 7898$ g mol^{-1} with PDI (M_w/M_n) = 1.17.

3. Results and discussion

3.1. Synthesis and characterization

Atom transfer radical polymerization (ATRP) has been proven to be a very powerful polymerization technique for the preparation of block copolymers from various monomers [24–27]. In this work, the styrene macroinitiator (**SMi**) [13] was used to copolymerize with methacrylate monomers containing biphenyl-4-ylthiophene (**M1**) and biphenyl-4-ylfluorene (**M2**) pendants to produce diblock copolymers. The

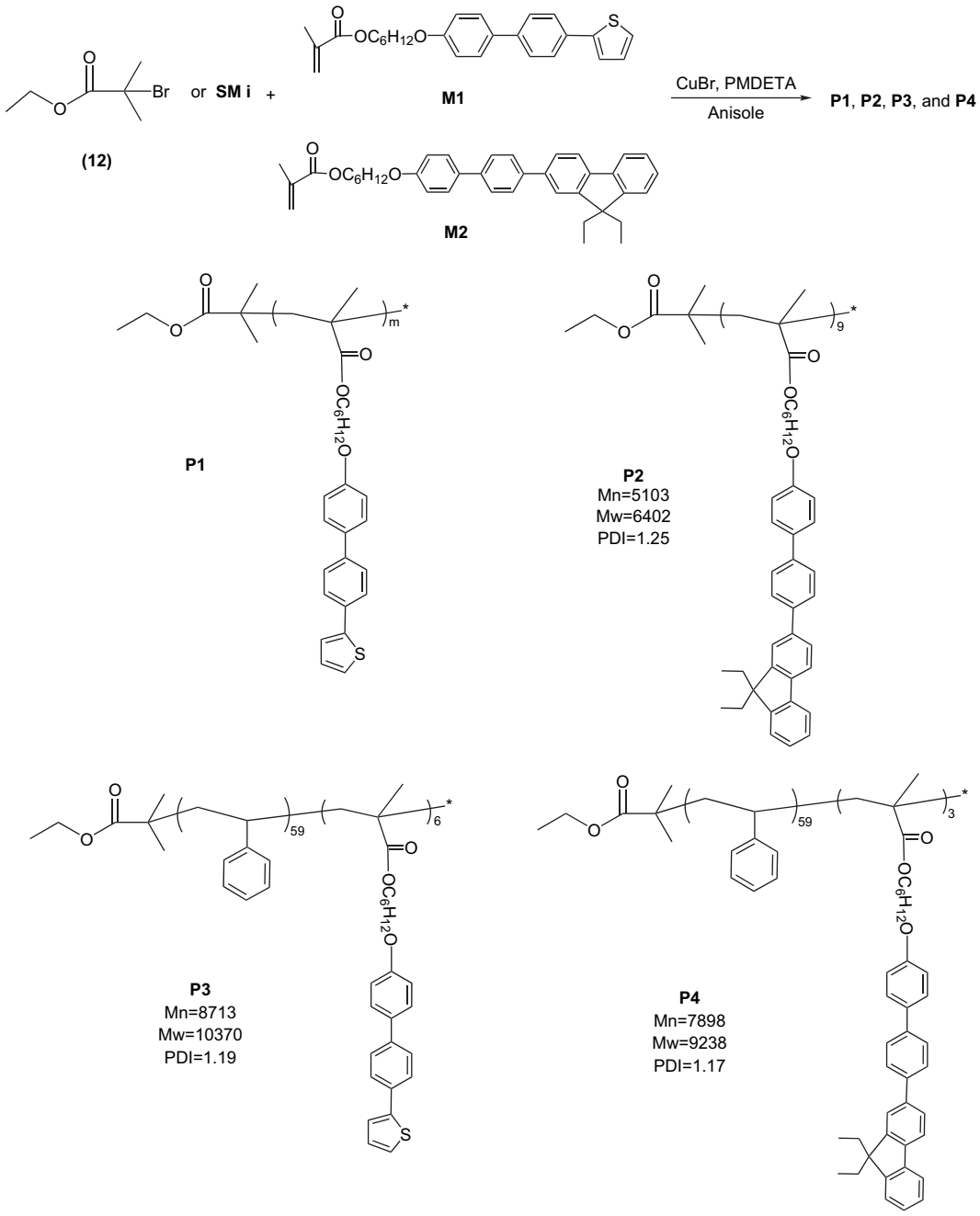

Scheme 2. Synthetic routes of homopolymers (**P1** and **P2**) and block copolymers (**P3** and **P4**).

number-average molecular weights (M_n) as well as PDI values of homopolymer (**P2**) and diblock copolymers (**P3** and **P4**) containing biphenyl-4-ylthiophene and biphenyl-4-ylfluorene LC blocks determined by GPC (THF as an eluant) are shown in Table 1. It indicates that all of the macroinitiator (**SMi**), homopolymer (**P2**), and diblock copolymers (**P3** and **P4**) with extended molecular weights had small PDI values determined by ATRP. Due to the poor solubility of longer biphenyl-4-ylthiophene units in **P1**, homopolymer **P1** was unable to be characterized, including the molecular weight. According to the number-average molecular weight (M_n) of homopolymer **P2**, i.e. 5103 g mol^{-1} with a PDI value of 1.25, homopolymer **P2** contains only about 9 units of biphenyl-4-ylfluorene monomer

Table 1
Molecular weight and thermal properties of polymers **P1**–**P4**

Sample	M_n (g mol^{-1})	M_w (g mol^{-1})	PDI (M_w/M_n)	T_d[a] (°C)	T_g[b] (°C)
P1[c]	–[c]	–[c]	–[c]	315	187.2
P2	5103	6402	1.25	338	81.3
P3[d]	8713	10,370	1.19	349	91.3
P4[d]	7898	9238	1.17	333	90.6

[a] Temperature of 5% weight loss measured by TGA under nitrogen.
[b] The glass transition temperatures (°C) were determined by DSC (with a heating and cooling rate of 5 °C/min).
[c] The molecular weight was undetermined since polymer **P1** is insoluble in most organic solvents.
[d] The number-average molecular weight (M_n) of macroinitiator **SMi** determined by GPC was 6196 g mol^{-1} with a PDI value of 1.11.

(**M2**). In addition, the number-average molecular weight (M_n) of macroinitiator (**SMi**) determined by GPC was 6196 g mol^{-1} (containing about 59 styrene monomer units) with a PDI value of 1.11, so diblock copolymers **P3** and **P4** only contain about 6 and 3 units of methacrylate monomers consisting of biphenyl-4-ylthiophene (**M1**) and biphenyl-4-ylfluorene (**M2**) pendants, respectively, as shown in the chemical structures of Scheme 2.

3.2. Thermal and mesogenic properties

The thermal stabilities of polymers (**P1**–**P4**) under an atmosphere of nitrogen were evaluated by thermogravimetric analysis (TGA), which indicates that the values of T_d (the degradation temperature of 5% weight loss in nitrogen) $\geq$ 315 °C for all polymers (as shown in Table 1). Due to the unclear glass transition temperatures (T_gs) of these block copolymers, T_g values were only detectable during the first heating scans of DSC measurements (with a heating rate of 5 °C/min) by following the quench of polymers (from 200 °C) in liquid nitrogen. By this quenching process, the T_g values of all polymers in DSC measurements were demonstrated more clearly in the range of 81–187 °C as shown in Table 1 and Fig. 1. Comparing polymers **P1** and **P2**, they exhibited glass transition temperatures (T_gs) at 187 and 81 °C, correspondingly. **P1** was more rigid than **P2** due to no lateral flexible chains on the pendants of **P1** and thus to have poorer solubility. Therefore, the T_g value of **P1** was higher than that of **P2**. However, the T_g values of block copolymers **P3** and **P4** were comparable (around 91 °C), which were mostly contributed from the flexible blocks of polystyrene (PS) [28,29] due to the longer block, i.e. larger molecular weight, of PS originated from macroinitiator **SMi**.

The mesogenic properties of all polymers were characterized by polarizing optical microscopy (POM) and differential scanning calorimetry (DSC). The phase transition temperatures and enthalpies of polymers **P1**–**P4** are summarized in Table 2 and their DSC thermograms are displayed in Fig. 1. To avoid thermal decomposition, these polymers were only heated up to about 300 °C (with a heating rate of 5 °C/min). Since both monomers, i.e. biphenyl-4-ylthiophene monomer (**M1**) and biphenyl-4-ylfluorene monomer (**M2**), possess the smectic A and nematic phases, respectively, polymers **P1**–**P4** indeed inherit the LC properties from their constituents (**M1** and **M2**). Regarding their mesomorphism, homopolymer **P1** and block copolymer **P3** which contain biphenyl-4-ylthiophene units possessed the smectic A phase. **P2** and **P4** were amorphous polymers with T_g = 81 and 91 °C, respectively. Homopolymer **P2** showed a stable glass-forming nematic phase, but **P4** did not possess any mesogenic phase due to a less monomer content (**M2**) of biphenyl-4-ylfluorene units in the copolymer composition of **P4**. Fig. 2 shows a fan-shaped focal conic texture of homopolymer **P1** observed by POM (at 255 °C cooling), which is a characteristic texture of the smectic A phase. In addition, their smectic phases had been further confirmed by X-ray diffraction (XRD) measurements (will be described later). Because of no lateral flexible chains on the thiophene pendants of **P1** and **P3**, rigid rods of LC blocks generate stronger transverse interaction and thus induce the smectic phases in polymers **P1** and **P3**. Interestingly, even though block copolymer **P3** contains only about 6 biphenyl-4-ylthiophene monomer units (**M1**) and 59 styrene monomer

Table 2
Phase behavior of polymers **P1**–**P4**[a–c]

Sample	Transition temperature (°C) and enthalpy (in parentheses, kJ/g)	T_i[d] (°C)
P1	**K** 235.4 (15.8) $\mathbf{S_A}$	~270
P2	**G** 81.3 **N**	~140
P3	**K** 218.9 (4.1) $\mathbf{S_A}$	~275
P4	**G** 90.6	~145

[a] Transition temperatures (°C) and enthalpies (in parentheses, kJ/mol) were determined by DSC (a heating rate of 5 °C/min).
[b] **G** = glass temperature; **K** = crystalline; **N** = nematic; $\mathbf{S_A}$ = smectic A.
[c] Transition temperatures of **M1** and **M2** are as follows: **M1**: **K** 185.3 °C (52.2 kJ/g) $\mathbf{S_A}$ with T_i = 245 °C; **M2**: **K** 60.4 °C (3.4 kJ/g) **N** with T_i = 98 °C.
[d] T_i: all isotropization temperatures, including monomers **M1** and **M2**, were characterized by polarizing optical microscopy (POM).

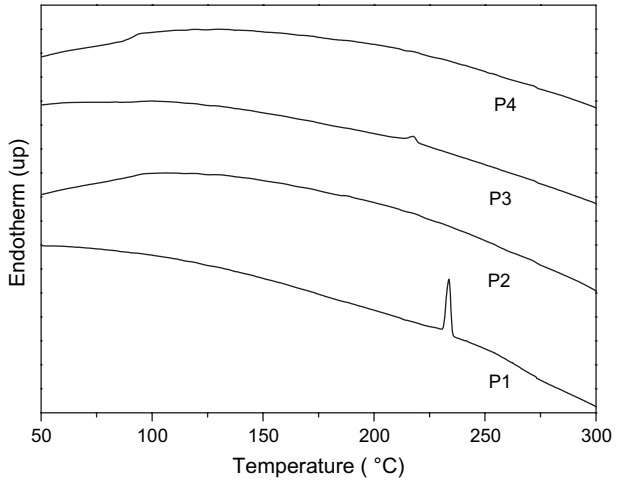

Fig. 1. DSC thermograms of polymers **P1**–**P4** during the first heating scan at 5 °C/min.

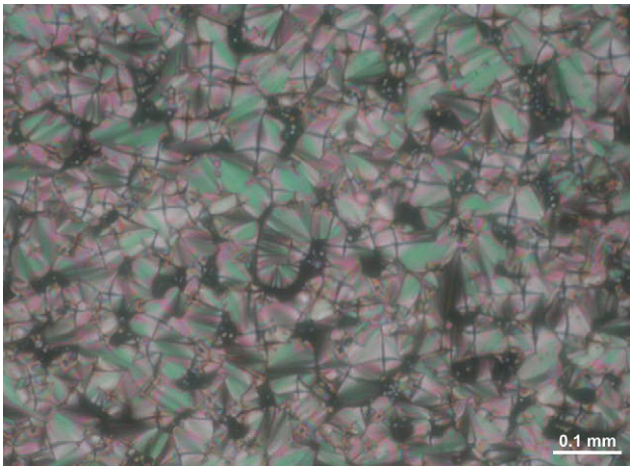

Fig. 2. POM texture of the mesophase (S_A) of polymer **P1** observed at 255 °C (cooling).

Table 3
XRD diffraction data of polymers **P1** and **P3**

Sample	Mesophase	Temperature (°C)	*d*-Spacing[a] (Å)
P1	$\mathbf{S_A}$	255	$d_{001} = 26.98$ $d_{002} = 13.68$
P3	$\mathbf{S_A}$	230	$d_{001} = 26.86$

[a] The theoretical *d*-spacing value is 23.7 Å for polymers **P1** and **P3**.

units, **P3** still can sustain its mesogenic property ascribed to the rigid thiophene pendants of the short block (6 monomer units). Regarding homopolymer **P2**, the lateral diethyl groups on 9-position of fluorene pendants, which separate the rigid cores of the side-chains, cause the reduction of transverse interaction among rigid rods in **P2** and thus favor the nematic phase. However, in contrast to polymers **P1**–**P3**, block copolymer **P4** contains only about 3 biphenyl-4-ylfluorene monomer units (**M2**) but with 59 styrene monomer units, so it led to no mesogenic phase in **P4** due to the less rigidity and shorter block of biphenyl-4-ylfluorene LC units. Moreover, polymers **P1** and **P3** with thiophene pendant groups revealed higher isotropization temperatures (T_i around 270 °C) than polymers **P2** and **P4** with fluorene pendant groups (T_i around 140 °C). Therefore, the comparison of isotropization temperatures in monomers **M1**–**M2** and polymers **P1**–**P4** additionally suggests that the rigidity of biphenyl-4-ylthiophene units is higher than that of biphenyl-4-ylfluorene units.

3.3. X-ray measurements

In order to elucidate the structures of the mesophases, X-ray diffraction (XRD) measurements were carried out in the temperature ranges of mesophases for polymers **P1**–**P4**, and the XRD data are summarized in Table 3. Owing to no smectic phases in **P2** (only the nematic phase) and in **P4** (no mesophase), there are no any peaks in the XRD patterns of polymers **P2** and **P4**. As shown in Fig. 3, the XRD patterns of polymers **P1** and **P3** are almost identical and their layer *d*-spacing values are around 29 Å, which were attributed to the layer *d*-spacing in the rigid blocks of biphenyl-4-ylthiophene units. In addition, the layer *d*-spacing values in the ratio of 1:1/2 indicate lamellar orders exist in the mesophases of **P1** and **P3**. According to the molecular modeling calculation, the layer *d*-spacing value of coplanar structure in **M1** is about 23.7 Å. Therefore, the layer *d*-spacing value of 29 Å by XRD measurements in polymers **P1** and **P3** was suggested to be interdigitated packing of biphenyl-4-ylthiophene units in rigid blocks. By this evidence, the layered structures of polymers **P1** and **P3** have little relationship with respect to the flexible blocks of polystyrene (PS).

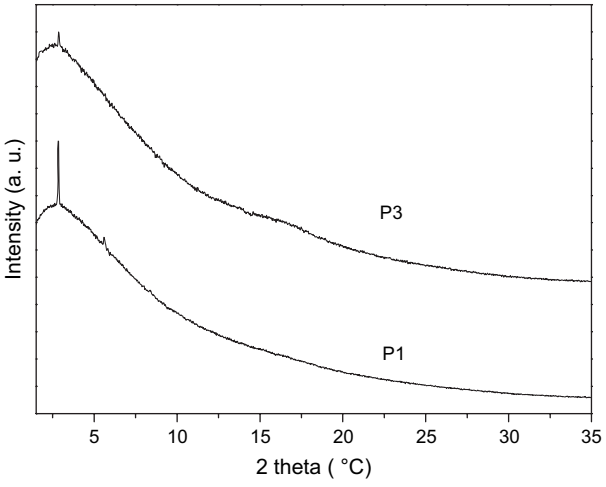

Fig. 3. X-ray diffraction patterns of polymers **P1** and **P3**.

Table 4
UV–visible absorption and photoluminescence spectral data of monomers (**M1** and **M2**) and polymers (**P1**–**P4**)

Sample	$\lambda_{max,Abs}$[a] (nm)	$\lambda_{max,PL}$[a] (nm)	Φ[b] (%)
M1	312	375	17.5
M2	322	385	23.2
P1	313	377	15.3
P2	321	386	19.0
P3	312	378	15.8
P4	321	387	18.9

[a] Absorption and PL spectra were recorded in dilute THF solutions at room temperature.
[b] PL quantum yield in THF and 9,10-diphenylanthrance was the reference of the quantum yield.

3.4. Photophysical properties

The photophysical properties, including the UV–visible absorption and photoluminescence (PL) spectral data, of all polymers in THF solutions are summarized in Table 4. Due to the identical rigid cores of luminescent biphenyl-4-ylthiophene units in monomer **M1** and polymers **P1** and **P3**, they have almost the same maximum absorption wavelength around 312 nm and emit blue light at approximately $\lambda_{max,PL} = 377$ nm in solutions. Comparably, monomer **M2** and polymers **P2** and **P4** have the identical rigid cores of luminescent biphenyl-4-ylfluorene units, therefore, they have almost the same values

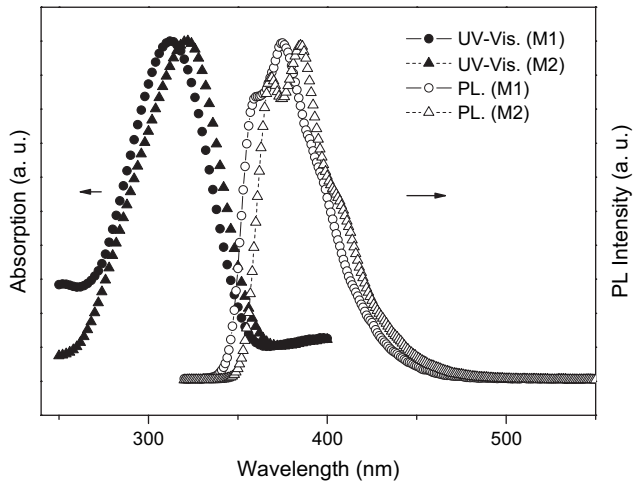

Fig. 4. UV–visible absorption (solid lines) and PL (dashed lines) spectra of monomers **M1** and **M2** in solutions (THF as solvent).

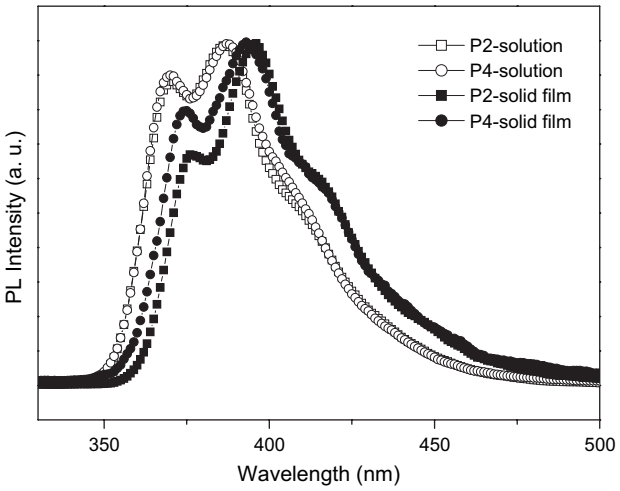

Fig. 5. PL spectra of polymers **P2** and **P4** in solid films and solutions (THF as solvent).

of the maximum absorption wavelength around 322 nm and the maximum PL wavelength ($\lambda_{max,PL}$) around 386 nm in solutions.

Fig. 4 shows the UV–visible absorption and PL spectra of monomers **M1** and **M2** in solutions. Compared with **M1**, monomer **M2** consisting of fluorene units results in longer maximum absorption wavelengths and PL wavelengths due to longer conjugation lengths in rigid cores. By the same reason, the maximum absorption and PL wavelengths of polymers **P2** and **P4** are more red-shifted than those of polymers **P1** and **P3**. Because of the less aggregated form originated from the lateral diethyl groups on fluorene pendants in **M2**, the quantum yield of biphenyl-4-ylfluorene monomer **M2** is higher than that of biphenyl-4-ylthiophene monomer **M1**. Accordingly, the quantum yields of polymers **P2** and **P4** are larger than those of polymers **P1** and **P3**.

Due to the poor solubility of polymers **P1** and **P3** and lower molecular weights of monomers **M1** and **M2**, the photophysical properties of these compounds in solid films were not

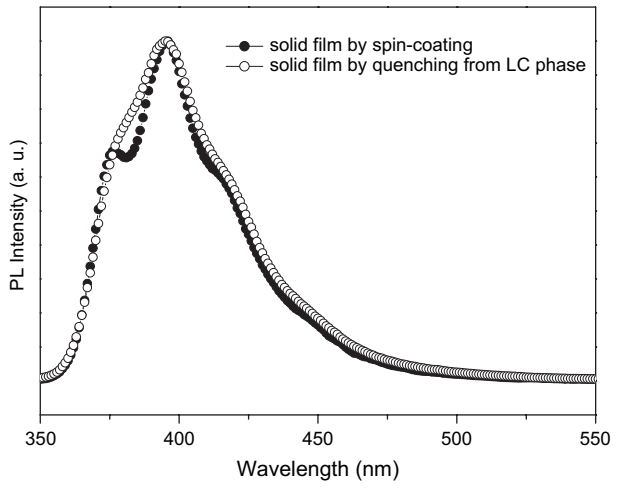

Fig. 6. PL spectra of **P2** solid films by spin-coating and quenching (by liquid N_2) from 130 °C (the nematic phase).

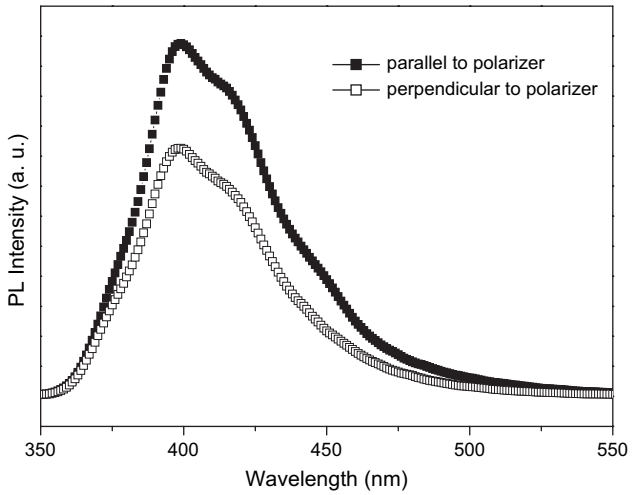

Fig. 7. Polarized PL spectra of aligned **P2** solid film by quenching from 130 °C on a rubbing PI substrate, where $PL_{\parallel}$ is the parallel PL intensity as the polarizer is parallel to the rubbing direction, and $PL_{\perp}$ is the perpendicular PL intensity as the polarizer is perpendicular to the rubbing direction.

obtained. Compared with solutions, solid films of polymers **P2** and **P4** in Fig. 5 exhibit red-shifted PL emissions around 396 nm owing to the π–π* aggregation of the rigid cores. In addition, the differences of photophysical properties between polymers **P2** and **P4** (both in solutions and solid films) are trivial, so the flexible PS blocks did not reflect important contribution to the photophysical properties. Fig. 6 displays the PL spectra of **P2** solid films by spin-coating and quenching (by liquid N_2) from 130 °C (the nematic phase). Due to the frozen nematic structure by quenching, **P2** was more orderly aligned and it led to aggregation of rigid cores in Fig. 6. Hence, the shorter wavelength peak at 376 nm in PL spectrum of **P2** solid film became a shoulder by quenching, which is similar to our previous report [7]. In order to evaluate the effect of mesogenic structure on photoluminescence properties, polarized PL spectra (as shown in Fig. 7) were measured from aligned **P2** solid film by quenching from 130 °C on a rubbing PI substrate. Polarization ratio ($PL_{\parallel}/PL_{\perp}$) was about 1.43, where $PL_{\parallel}$ is the maximum PL emission intensity as the polarizer is parallel to the rubbing direction, and $PL_{\perp}$ is the maximum PL emission intensity as the polarizer is perpendicular to the rubbing direction. This result shows the effect of mesogenic alignment of **P2** on rubbing PI substrate can induce a polarized PL emission with a polarization ratio of 1.43.

4. Conclusions

- Atom transfer radical polymerization (ATRP) was employed to fabricate block copolymers consisting of PS macroinitiators and liquid crystalline polymethacrylate blocks containing biphenyl-4-ylthiophene (**M1**) and biphenyl-4-ylfluorene (**M2**) units.
- Thermal and XRD investigations indicate that polymers **P1** and **P3** exhibited the interdigitated smectic A phase which has little relationship with respect to their flexible PS blocks.

- In terms of PL wavelengths of all block copolymers in dilute solutions, **P2** and **P4** are more red-shifted than **P1** and **P3**, which might be due to longer conjugation lengths of the lateral biphenyl-4-ylfluorene blocks in polymers **P2** and **P4**.
- The shorter wavelength peak at 376 nm in PL spectrum of **P2** solid film became a shoulder by quenching from 130 °C (the nematic phase). The effect of mesogenic alignment of **P2** on rubbing PI substrate can induce a polarized PL emission with a polarization ratio of 1.43.

Acknowledgements

We are grateful for the financial support provided by the National Science Council of Taiwan (ROC) through NSC 94-2113-M-009-005. The powder XRD measurements were supplied by beamline BL17A (charged by Dr. Jey-Jau Lee) of the National Synchrotron Radiation Research Center (NSRRC) in Taiwan.

References

[1] Osuji CO, Chen JT, Ober CK, Thomas EL. Polymer 2000;41:8897.
[2] Park C, Yoon J, Thomas EL. Polymer 2003;44:6725.
[3] Poser S, Fischer H, Arnold M. J Polym Sci Part A Polym Chem 1996;34:1733.
[4] Kihara H, Kishi R, Miura T, Kato T, Ichijo H. Polymer 2001;42:1177.
[5] Yu H, Shishido A, Ikeda T, Iyoda T. Macromol Rapid Commun 2005;26:1594.
[6] Minich EA, Nowak AP, Deming TJ, Pochan DJ. Polymer 2004;45:1951.
[7] Lin HC, Lee KW, Tsai CM, Wei KH. Macromolecules 2006;39:3808.
[8] Gopalan P, Li X, Li M, Ober CK, Gonzales CP, Hawker CJ. J Polym Sci Part A Polym Chem 2003;41:3640.
[9] Hawker CJ, Wooley KL. Science 2005;309:1200.
[10] Tew GN, Aamer KA, Shunmugam R. Polymer 2005;46:8440.
[11] Denizli BK, Lutz JF, Okrasa L, Pakula T, Guner A, Matyjaszewski K. J Polym Sci Part A Polym Chem 2005;43:3440.
[12] Li XG, Huang MR, Guan GH, Sun T. J Appl Polym Sci 1997;66:2129.
[13] Li XG. J Appl Polym Sci 1999;73:2921.
[14] Tang W, Li XG, Yan D. J Appl Polym Sci 2004;91:445.
[15] Tian Y, Watanabe K, Kong X, Abe J, Iyoda T. Macromolecules 2002;35:3739.
[16] Schneider A, Zanna JJ, Yamada M, Finkelmann H, Thomann R. Macromolecules 2000;33:649.
[17] He X, Zhang H, Yan D, Wang X. J Polym Sci Part A Polym Chem 2003;41:2854.
[18] Figueiredo P, Gronski W, Bach M. Macromol Rapid Commun 2002;23:38.
[19] Özbek H, Yıldız S, Pekcan Ö, Hepuzer Y, Yagci Y, Galli G. Mater Chem Phys 2002;78:318.
[20] Hepuzer Y, Serhatli IE, Yagci Y, Galli G, Chiellini E. Macromol Rapid Commun 2002;202:2247.
[21] Anthamatten M, Wu JS, Hammond PT. Macromolecules 2001;34:8574.
[22] Sänger J, Gronski W, Maas S, Stuhn B, Heck B. Macromolecules 1997;30:6783.
[23] Anthamatten M, Zheng WY, Hammond PT. Macromolecules 1999;32:4838.
[24] Lee KW, Wei KH, Lin HC. J Polym Sci Part A Polym Chem 2006;44:4593.
[25] Gray GW, Harrison KJ, Nash JA. J Chem Soc Chem Commun 1974;431.
[26] Matyjaszewski K, Xia J. Chem Rev 2001;101:2921.
[27] Kamigaito M, Ando T, Sawamoto M. Chem Rev 2001;101:3689.
[28] Wang J, Mao G, Ober CK, Kramer EJ. Macromolecules 1997;30:1906.
[29] Schmalz H, Bolker A, Lange R, Krausch G, Abetz V. Macromolecules 2001;34:8720.